# CHAPTER IV

## CASE STUDY – A TEN-BAR TRUSS PROBLEM

Let us consider a two-dimensional, cantilevered truss with the geometry, supports and loading condition as shown in Figure 4.1. Each member of the truss is designated with a number in the range of 1–10. Each node is also designated with a number in the range of 1–6.

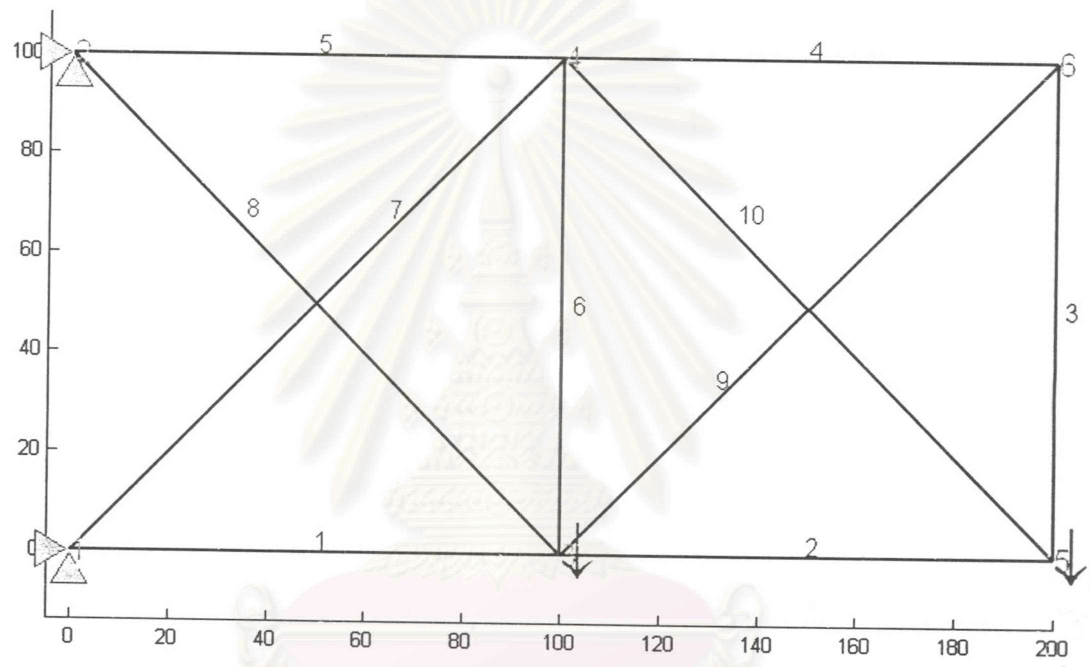


Figure 4.1 The geometry of the ten bar truss.

The length of all the horizontal and vertical members is 100cm. The length of the diagonal members is approximately 141cm. In the first part of the investigation, all members are assigned with the same cross-sectional area, 4.692cm$^2$, for nonlinear analysis. In the second part, the sizing optimization, the list of available cross-sectional areas is specified in accordance with the JIS G 3192 table, using the equal single angles section. As previously mentioned in Chapter 2, the equal single angles are very popular in the design of trusses, particularly light trusses. However, this is the kind of non-compact section in which the yield stress is unable to spread over the entire area of the compression member before buckling. Three types of buckling are possible for this section; however, the current investigation deals only with flexural buckling.

A typical variation of the ten-bar truss problem is the use of either discrete or continuous cross-sectional areas. For the current problem, a set of 20 discrete values are used for the possible cross-sectional areas for each member (1.427, 1.727, 2.336, 3.755, 3.492, 4.302, 3.892, 4.802, 5.644, 4.692, 5.802, 6.367, 7.527, 9.761, 8.127, 8.727, 12.69, 16.56, 9.327, and 10.55 cm$^2$). The radii of gyration (cm) corresponding to the above list are 0.747, 0.908, 1.230, 1.200, 1.360, 1.360, 1.530, 1.520, 1.500, 1.850, 1.840, 1.990, 1.980, 1.940, 2.140, 2.300, 2.250, 2.220, 2.460, and 2.770 cm, respectively.

The modulus of elasticity of 2,038,901.9 kg/cm$^2$ and the mass density of 7.849x10$^{-3}$ kg/cm$^3$ are used for steel. The minimum yield stress is 2531.0507 kg/cm$^2$ and the maximum deflection of any node in both the vertical and horizontal directions is 2.0cm (1% of the cantilever span or $\frac{L}{100}$).

The truss is subjected to two static point loads with downward direction as shown in the Figure 4.1.

## IV.1. Nonlinear analysis

### *IV.1.1 Linear elastic analysis*

The linear analysis of the truss is performed by setting the load ratio increment $\Delta\lambda$ = 1.0 and the number of re-analysis times as zero. The program is executed only one time, with the structure subjected to the entire given loads. The geometrical nonlinearity is neglected. The material nonlinearity is also disregarded by using a constant modulus of elasticity to simulate the linear elastic analysis for the given truss.

The absolute value of the load is 2268 kgf. The self-weight load factor is $\phi_D = 1.2$ and the live load factor is $\phi_L = 1.6$. The direction of the load is as shown in Figure 4.1. All the truss members are assigned with the same cross-sectional area of 4.692cm$^2$, the tenth entry in the list of possible cross-sectional areas.

It can be seen in Figure 4.2 that the load ratio in this case is constant with $\lambda_{min}$ = $\lambda_{max}$ = 1. This means that the analysis is performed only once, and the truss passes the checking criteria. The displacement and stress outputs are summarized in Table 4.1. Figure 4.3 illustrates the deformed shape of the truss.

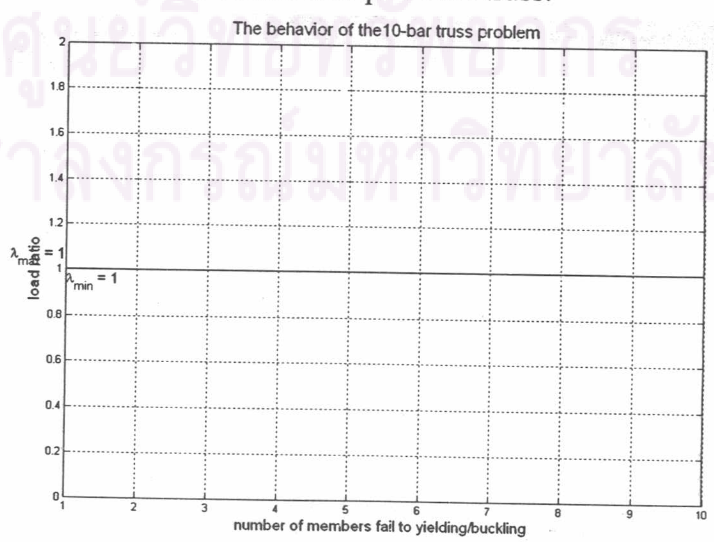


Figure 4.2 The constant load ratio of the ten-bar truss in linear elastic analysis.

Table 4.1 The displacement and axial stress results from the linear elastic analysis.

| Linear Elastic Analysis | | | |
|---|---|---|---|
| Dof. No. | Displacement (cm) | Element No. | Stress (kg/cm$^2$) |
| 1 | 0.000 | 1 | -3180.80 |
| 2 | 0.000 | 2 | -928.18 |
| 3 | 0.000 | 3 | 620.49 |
| 4 | 0.000 | 4 | 623.59 |
| 5 | -0.156 | 5 | 3034.20 |
| 6 | -0.382 | 6 | 548.67 |
| 7 | 0.149 | 7 | -2099.30 |
| 8 | -0.355 | 8 | 2300.40 |
| 9 | -0.201 | 9 | -882.22 |
| 10 | -0.834 | 10 | 1314.10 |
| 11 | 0.180 | | |
| 12 | -0.804 | | |

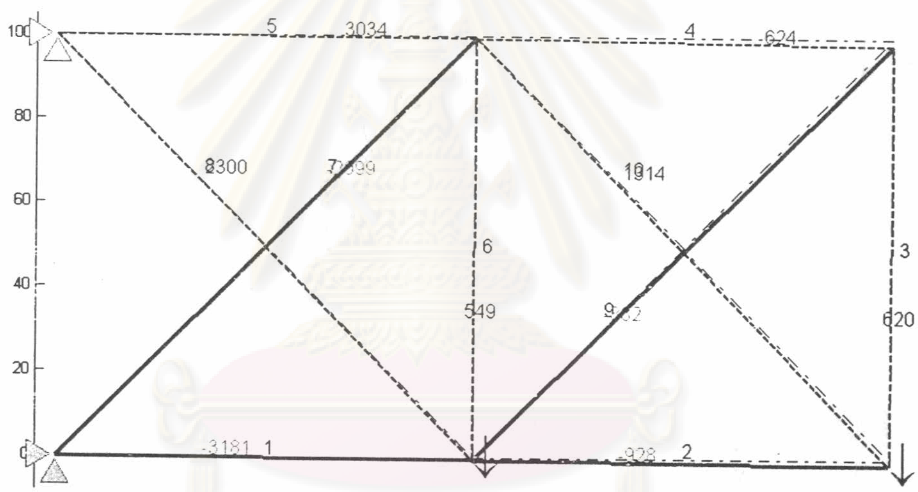


Figure 4.3 The graphical representation of the truss displacements from the linear elastic analysis.



*IV.1.2 Nonlinear analysis*

In this case, the truss is analyzed taking into account the material and geometrical nonlinearities. The load ratio increment $\Delta\lambda = 0.04$ is used in the analysis.

The absolute value of the load remains the same as for the previous case at 2268 kgf. Again, the self-weight load factor is $\phi_D = 1.2$ and the live load factor is $\phi_L = 1.6$. All the members are assigned with the same cross-sectional area of 4.692cm$^2$.

Figure 4.4 shows the load ratio history for the ten-bar truss. It is observed that the first member fails at $\lambda_{min} = 1.24$, and the truss reaches its maximum allowable displacement at $\lambda_{max} = 2.9$.

The displacements and stresses from the nonlinear analysis is summarized in Table 4.2 and the deformed shape of the truss is illustrated in figure 4.5. Comparing to the linear elastic analysis, the axial stresses of all members are distributed more evenly.

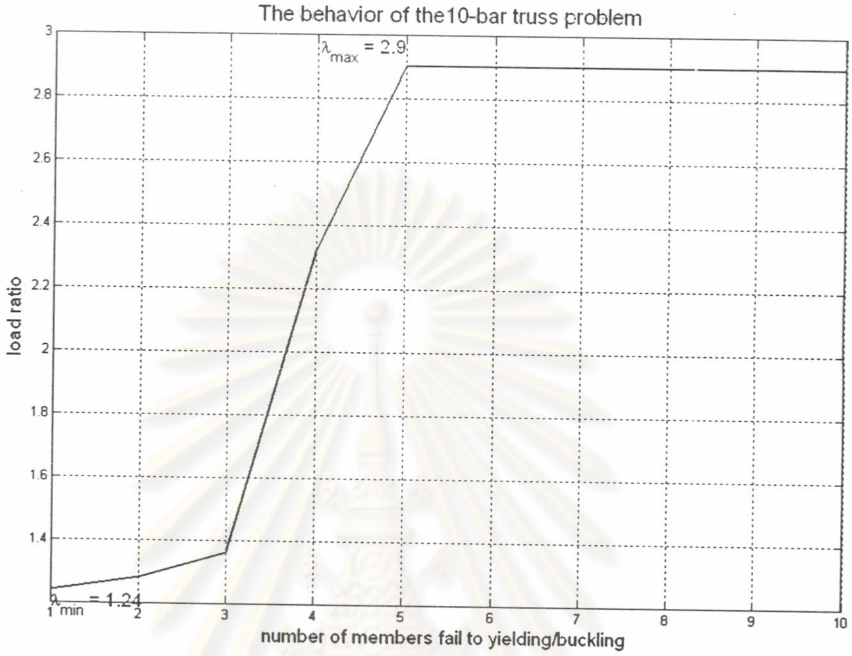


Figure 4.4 The load ratio history of the ten-bar truss in the nonlinear analysis.

Table 4.2 The displacement and axial stress results from the nonlinear analysis.

| Nonlinear Analysis | | | |
|---|---|---|---|
| Dof. No. | Displacement (cm) | Element No. | Stress (kg/cm$^2$) |
| 1 | 0.000 | 1 | -1875.20 |
| 2 | 0.000 | 2 | -1322.60 |
| 3 | 0.000 | 3 | 945.04 |
| 4 | 0.000 | 4 | 948.67 |
| 5 | -0.587 | 5 | 2296.50 |
| 6 | -0.868 | 6 | 1197.40 |
| 7 | 0.236 | 7 | -1617.10 |
| 8 | -0.809 | 8 | 2299.90 |
| 9 | -0.767 | 9 | -1343.10 |
| 10 | -1.997 | 10 | 1884.90 |
| 11 | 0.283 | | |
| 12 | -1.951 | | |

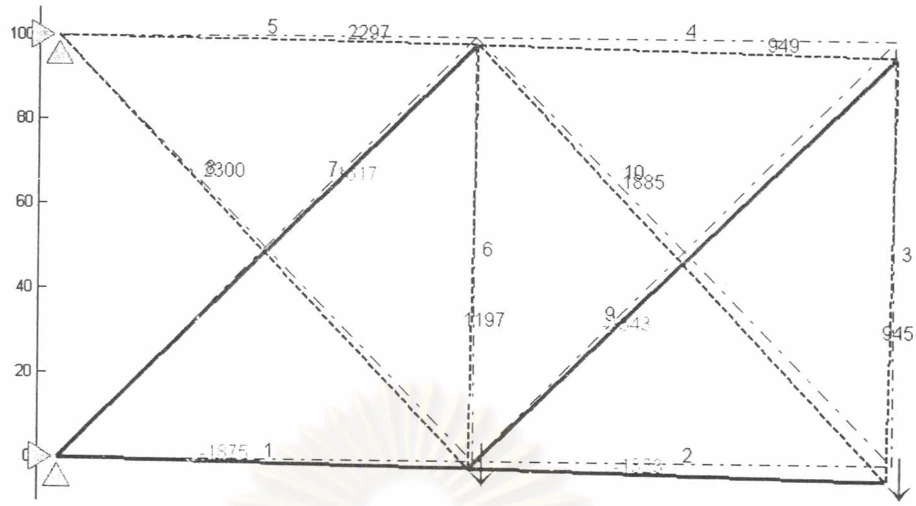


Figure 4.5 The graphical representation of the truss displacements from the nonlinear analysis.

*IV.1.3 Ultimate analysis*

For the present case the truss is also analyzed taking into account the material and geometrical nonlinearities with all the input parameters and conditions as in the previous case. However, this time the analysis is repeated many times until all the members of the truss fail. The final load ratio before the truss collapses is taken as the critical value.

Figure 4.6 shows the load ratio history of the truss. The first member fails at $\lambda_{min}$ = 1.24 (same as in the previous case) and the truss collapses at $\lambda_{max} \equiv \lambda_{critical}$ = 7.06, or at the load equal to $7.06\left[1.2D+1.6(2268)\right]$ kgf where D stands for the self weight of the truss.

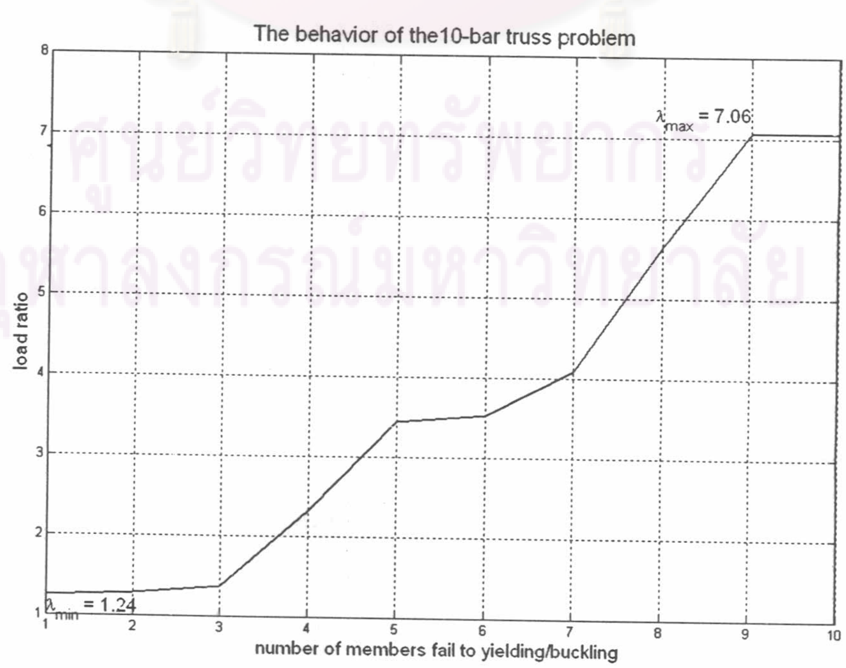


Figure 4.6 The load ratio history of the ten-bar truss in the ultimate analysis.

Table 4.3 summarizes the displacement and stress results and Figure 4.7 illustrates the deformed shape of the truss.

Table 4.3 The displacement and axial stress results from the ultimate analysis.

| Ultimate Analysis | | | |
|---|---|---|---|
| Dof. No. | Displacement (cm) | Element No. | Stress (kg/cm$^2$) |
| 1 | 0.000 | 1 | -1875.2 |
| 2 | 0.000 | 2 | -1848.1 |
| 3 | 0.000 | 3 | 2284.2 |
| 4 | 0.000 | 4 | 2275.6 |
| 5 | -1.411 | 5 | 2296.5 |
| 6 | -2.090 | 6 | 2290.8 |
| 7 | 0.568 | 7 | -1617.1 |
| 8 | -1.950 | 8 | 2299.9 |
| 9 | -1.843 | 9 | -1589.4 |
| 10 | -4.807 | 10 | 2282.7 |
| 11 | 0.679 | | |
| 12 | -4.695 | | |

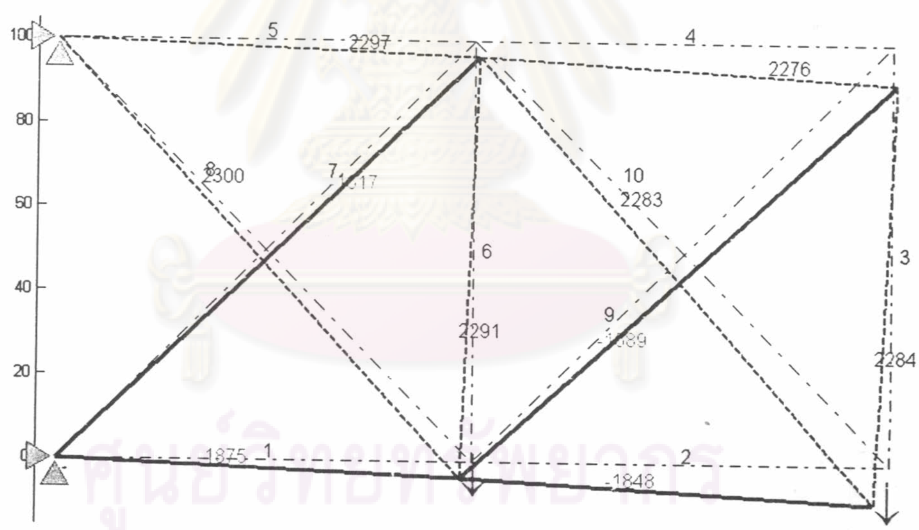


Figure 4.7 The graphical representation of the truss displacements from the ultimate analysis.

In order to capture the nonlinear behavior of the truss in more details, the load ratio increment $\Delta\lambda = 0.01$ is used and the analysis is repeated. The results are shown in Table 4.4 and Figures 4.8 – 4.9. It is seen that the nonlinear behavior of the truss can be captured more precisely in this case.

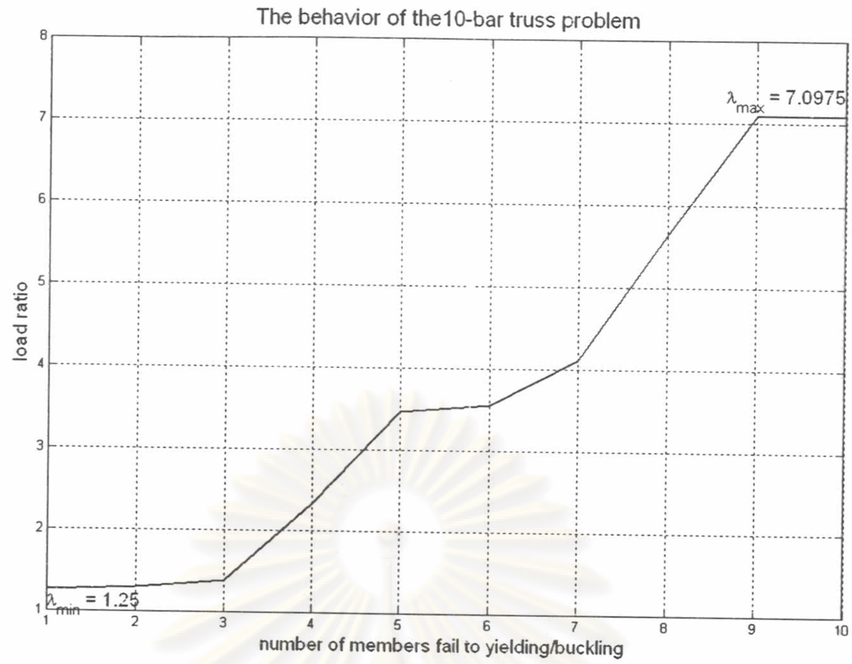


Figure 4.8 The load ratio history of the ten-bar truss in the ultimate analysis with $\Delta\lambda = 0.01$

Table 4.4 The displacement and axial stress results from the ultimate analysis with $\Delta\lambda = 0.01$

| Ultimate Analysis with $\Delta\lambda = 0.01$ | | | |
|---|---|---|---|
| Dof. No. | Displacement (cm) | Element No. | Stress ($kg/cm^2$) |
| 1 | 0.000 | 1 | -1845.9 |
| 2 | 0.000 | 2 | -1848 |
| 3 | 0.000 | 3 | 2281 |
| 4 | 0.000 | 4 | 2277.8 |
| 5 | -1.412 | 5 | 2280.1 |
| 6 | -2.092 | 6 | 2278.6 |
| 7 | 0.568 | 7 | -1592.7 |
| 8 | -1.952 | 8 | 2280.3 |
| 9 | -1.845 | 9 | -1584.8 |
| 10 | -4.812 | 10 | 2282.7 |
| 11 | 0.680 | | |
| 12 | -4.700 | | |

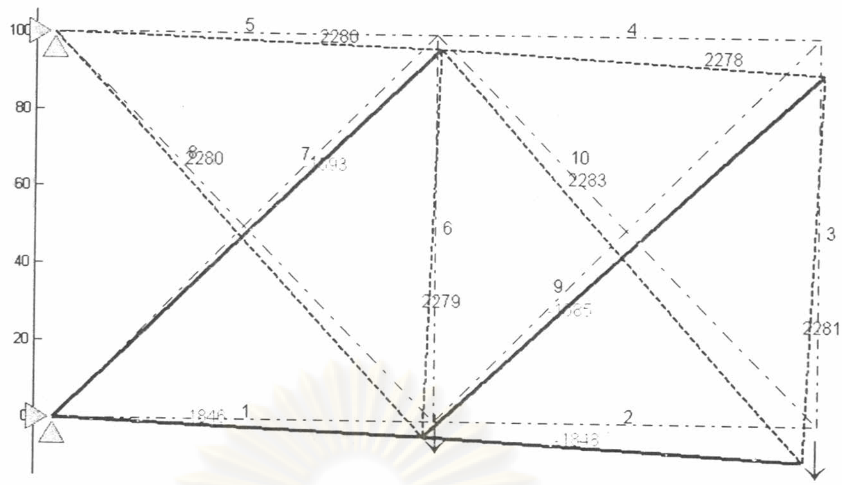


Figure 4.9 The graphical representation of the truss displacements from the ultimate analysis with $\Delta\lambda = 0.01$.

**IV.2. Sizing optimization using genetic algorithm**

There are many ways in which the parameters of the genetic algorithm can be adjusted. The optimum set of parameters may vary depending upon the specific characteristics of each problem. The current study selects the population size equal to 40 and the maximum number of generations at a sufficiently high value to allow the process to converge to the best possible solution.

In order to compare the optimization results with those of the previous analyses, the truss is again subjected to the medium load of 2268 kgf using the self-weight load factor of $\phi_D = 1.2$ and the live load factor of $\phi_L = 1.6$. The current investigation employs the load ratio increment $\Delta\lambda = 0.04$. This value is considered sufficient to examine the efficicacy of the proposed procedure.

*IV.2.1 Single-section optimization*

To ensure the reliability of the algorithm, all the members of the truss are assigned with a single section that can be selected from the list of twenty possible cross-sectional areas.

Figure 4.10 shows the optimization results. In the illustration, two points are plotted for each generation. The point showing a lower value of objective function represent the best solution and the point showing a higher value corresponds with the mean of the objective function for all the solutions in that generation.

The optimum cross-sectional area is found as 4.692 $cm^2$ (Figure 4.11), which coincides with the section in the nonlinear analysis.

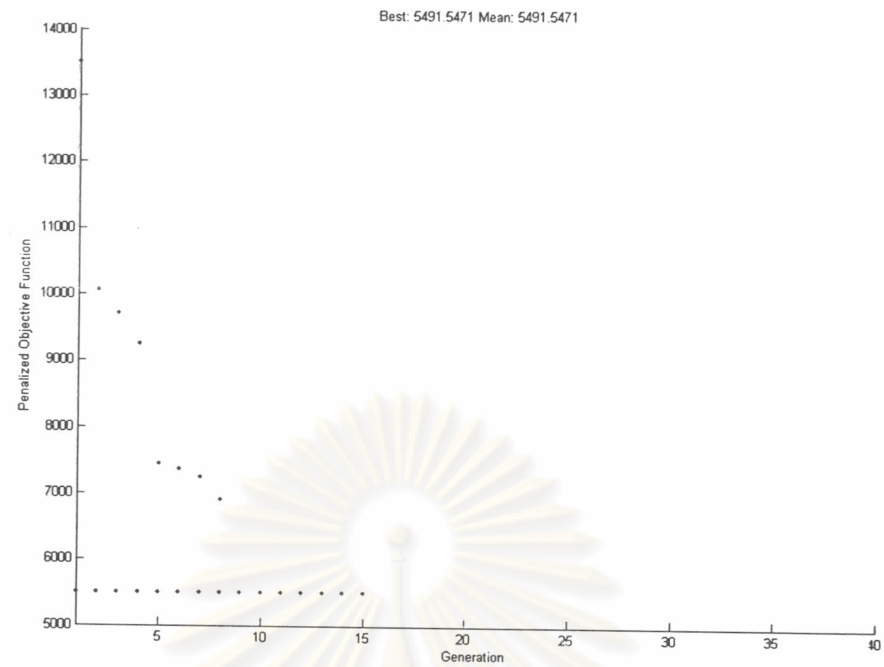


Figure 4.10 Convergence of the single-section optimization problem.

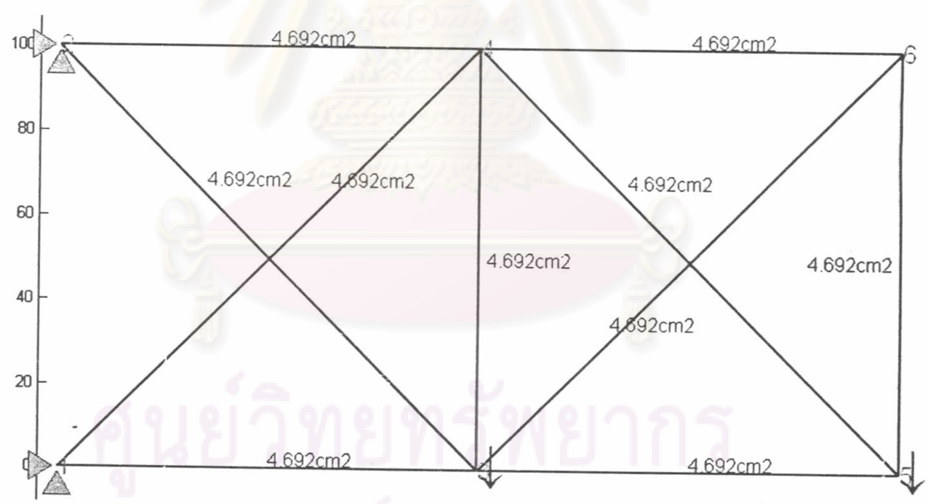


Figure 4.11 The section obtained for the single-section optimization problem.

*IV.2.2 Eight-section optimization*

In the previous case, all the truss members are assigned with the same cross-sectional area. In the present case, in order to examine the advantage of the algorithm, 8 different sections are used to form the list of available sections for the sizing optimization problem.

The cross-sectional areas of the 8 sections are 1.427, 1.727, 2.336, 3.755, 3.492, 4.302, 3.892 and 4.692 $cm^2$ with the corresponding radii of gyration of 0.747, 0.908, 1.230, 1.200, 1.360, 1.360, 1.500 and 1.850 cm, respectively.

Figure 4.12 shows the optimization results. In the illustration, two points are plotted for each generation. The point showing a lower value of objective function represent the best solution and the point showing a higher value correspond with the mean of the objective function for all the solutions in that generation (due to the large number of points, the set of the best points seems to be a continuous line in the figure).

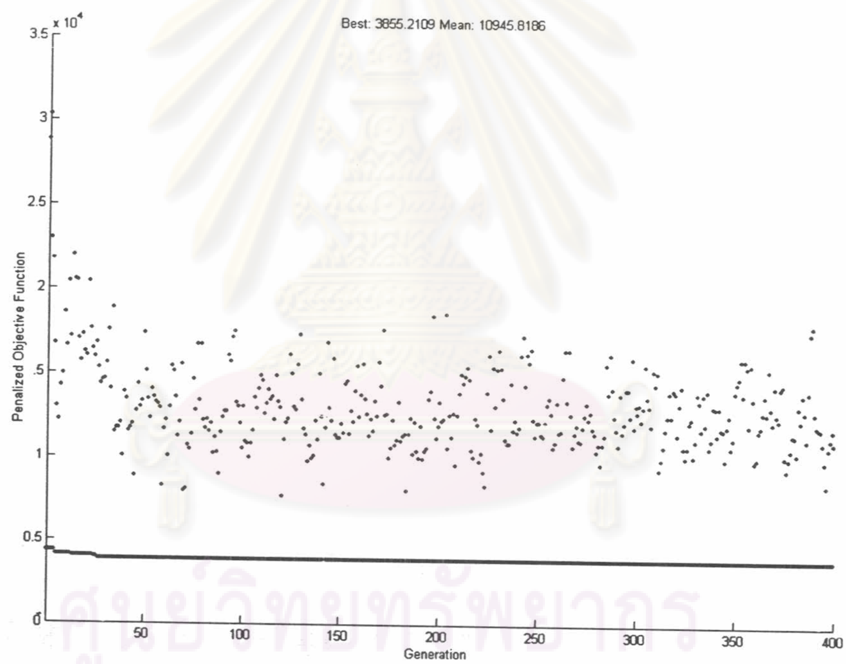


Figure 4.12 Convergence of the 8-section optimization problem.



It should also be noted that the penalty function $\theta_{2i}$ in equation (3.12) is modified in order to eliminate the case in which the initial load ratio is less than one by shifting the peak of the parabolic curve from 1.0 to 1.1, and neglecting the upper bound.

It is observed from Figure 4.13 that all the cross-sectional areas of the truss are less than or equal to 4.692 $cm^2$, the upper limit of the input sections. With this set of sections, $\lambda_{min}$ = 1.08 (>1.0) and the total volume of the truss is 3842.1 $cm^3$. This volume is approximately 70% compared with the previous case.

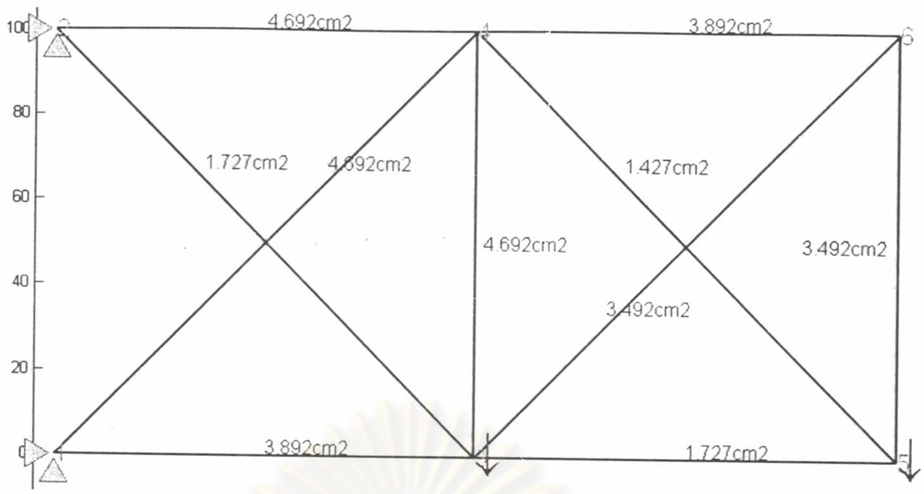


Figure 4.13 The sections obtained for the 8-section optimization problem.

*IV.2.3 Twenty-section optimization*

For the current case, all the 20 discrete values are used as the possible cross-sectional areas for the truss members (1.427, 1.727, 2.336, 3.755, 3.492, 4.302, 3.892, 4.802, 5.644, 4.692, 5.802, 6.367, 7.527, 9.761, 8.127, 8.727, 12.69, 16.56, 9.327, and 10.55 cm$^2$). The optimization results are summarized in Figure 4.14.

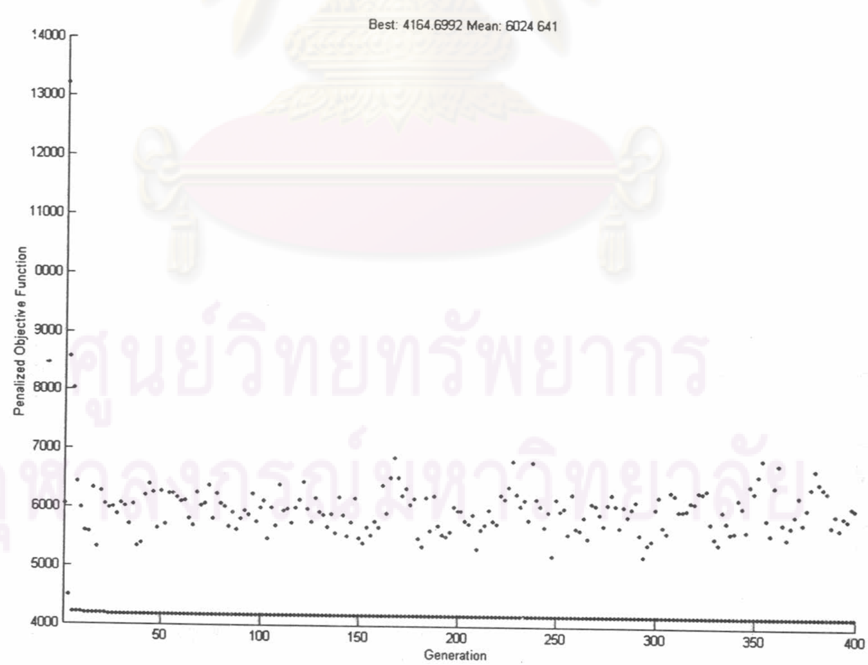


Figure 4.14 Convergence of the 20-section optimization problem.

The optimum cross-sectional areas for the truss members are illustrated in Figure 4.15.

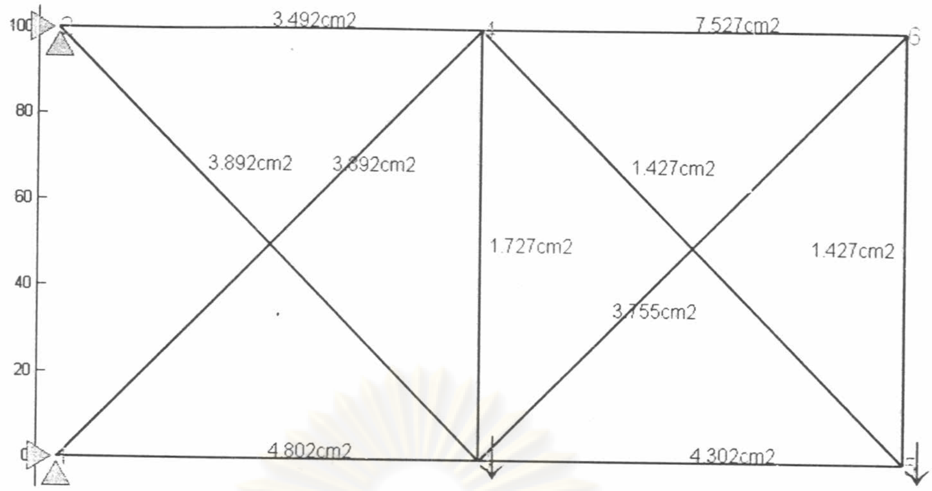


Figure 4.15 The sections obtained for the 20-section optimization problem.

With the set of sections in Figure 4.15, $\lambda_{min}$ = 1.08 and the total volume of the truss is 4161.4 $cm^3$. This volume is slightly higher compared with the eight-section case.